Dynamics of the Vertically Restrained Rocking Column

Michalis F. Vassiliou[1] and Nicos Makris, M.ASCE[2]

Abstract: This paper investigates the rocking response of a slender column that is vertically restrained with an elastic tendon that passes through its centerline. Following a variational formulation, the nonlinear equation of motion is derived, in which the stiffness and the prestressing force of the tendon are treated separately. In this way, the post-uplift stiffness of the system can be anywhere from negative to positive depending on the axial stiffness of the vertical tendon. This paper shows that vertical tendons are effective in suppressing the response of smaller columns subjected to long-period excitations. As the size of the column or the frequency of the excitation increases, the effect of the vertical tendon becomes immaterial given that most of the seismic resistance of large rocking columns originates primarily from the mobilization of their rotational inertia. **DOI: 10.1061/(ASCE)EM.1943-7889.0000953.** © *2015 American Society of Civil Engineers.*

Introduction

During the last two decades, there has been a growing effort to direct the attention of bridge engineers to the unique advantages associated with allowing bridge piers to uplift or, more generally, to rotate intentionally at specific locations by mobilizing a lower failure mechanism. In this way, the seismic demand on other critical locations of the structure is reduced while permanent displacements also remain small due to the inherent recentering tendency of the rocking mechanism.

In view of the appreciable damage to the hinge zones and the resulting permanent lateral displacements that are inherent to the current ductile, seismic-resistant design practice, Mander and Cheng (1999) introduced the damage avoidance design (DAD) in which the columns of a frame are allowed to rock on both the pile cap and the pier cap beam without inducing damage. This is achieved by terminating the longitudinal reinforcement of the columns before reaching the beam-column and the column-foundation interfaces. In the DAD, central post-tensioned steel tendons inside the columns are provided to increase the lateral resistance of the articulated structure. In fact, the force-deformation curve presented in Fig. 2.2 of the Mander and Cheng (1999) report indicates that the axial stiffness of the steel tendons is large enough that the post-uplift stiffness of the rocking frame is positive. By introducing such a stiff tendon that reverses the negative stiffness associated with rocking, one creates a stronger system; nevertheless, at present, it is not well understood to what extent a stiff vertical tendon that offers a positive lateral stiffness enhances the seismic stability of a tall rocking pier. A subsequent publication by Cheng (2008) presented shaking table test results from the seismic response of a two-column rocking frame with vertical restrainers. The effect of the various parameters of the system was examined in detail, and although some configurations in the Cheng (2008) study exhibited negative stiffness (i.e., R30PNK250 test), the physical significance and the effect of increasing the stiffness of the tendon were not discussed.

The pressing need for bridges to recenter after a strong seismic event motivated several studies (Priestley and Tao 1993; Palermo et al. 2005; Cheng 2007; Mahin et al. 2006; Sakai et al. 2006; Kam et al. 2010) that invariably use the basic concept of post-tensioning the bridge piers with vertical tendons while reducing or even terminating the longitudinal reinforcement of the columns before reaching their bottom and top interfaces, as was originally proposed by Mander and Cheng (1999). The same concept receives attention in the prefabricated bridge technology, where again the bridge piers are connected to the foundation and the deck with vertically post-tensioned tendons that pass through the axis of the column together with a lighter longitudinal mild-steel reinforcement that runs near the circumference of the columns (Wacker et al. 2005; Cohagen et al. 2008). With this design, during earthquake loading, the majority of deformation is concentrated at the interface between the pier and the foundation and at the interface between the pier and the cap beam. The overall deformation pattern of the post-tensioned frame resembles the deformation pattern of the free-standing rocking frame (Makris and Vassiliou 2013, 2014). Nevertheless, the prevailing practice at present is to offer enough lateral moment resistance to the hybrid rocking frame so that its lateral stiffness is invariably positive. The same concept has been applied to buildings by using beams prestressed with unbonded tendons (Pampanin 2005; Christopoulos et al. 2002).

More than a decade ago, Makris and Zhang (2001) and Makris and Black (2002) investigated the rocking response and overturning of rigid blocks and equipment anchored with brittle restrainers, and concluded that vertical restrainers are more effective in preventing overturning of small blocks when subjected to low-frequency pulses. As the size of the column increases, the rotational inertia of the free-standing single column increases with the square of its size, and the seismic stability of large, free-standing columns originates primarily from the difficulty to mobilize their large rotational inertia, rather than from the marginal effect of the restrainers. Part of the motivation of this study is to build upon the previously referenced work and bring forward that the ample seismic resistance of tall rocking columns originates primarily from the difficulty to mobilize their rotational inertia, whereas the effect of the restraining vertical tendon becomes increasingly marginal as the size of the rocking column increases.

[1]Postdoctoral Researcher, Institute of Structural Engineering, Swiss Federal Institute of Technology, Zürich, Switzerland; formerly, Ph.D. Student, Dept. of Civil Engineering, Univ. of Patras, Patras, Greece (corresponding author). E-mail: vassiliou@ibk.baug.ethz.ch; mfvassiliou@gmail.com

[2]Professor, Dept. of Civil Engineering, Division of Structures, Univ. of Patras, GR-26500 Patras, Greece.

Note. This manuscript was submitted on May 9, 2014; approved on March 3, 2015; published online on May 19, 2015. Discussion period open until October 19, 2015; separate discussions must be submitted for individual papers. This paper is part of the ***Journal of Engineering Mechanics***, © ASCE, ISSN 0733-9399/04015049(10)/$25.00.

Notable Limitation of the Equivalent Static Lateral Force Analysis

Seismic Resistance of Free-Standing Columns under Equivalent Static Lateral Loads

Consider a free-standing rigid column with size $R = \sqrt{b^2 + h^2}$ and slenderness $(b/h) = \tan\alpha$ as shown in Fig. 1(a). Let the base of the column move (say to the left) with a *slowly* increasing acceleration, $\ddot{u}_g$ (say a very long-duration acceleration pulse that allows for an equivalent static analysis). Uplift of the block (recentering moment; mgb) happens when the seismic demand (overturning moment; $m\ddot{u}_g h$) reaches the seismic resistance (recentering moment; (mgb). When uplifting is imminent, *static* moment equilibrium of the block about the pivoting point O gives

$$\underbrace{m\ddot{u}_g h}_{\text{demand}} = \underbrace{mgb}_{\text{resistance}} \quad \text{or} \quad \underbrace{\ddot{u}_g}_{\text{demand}} = g\frac{b}{h} = \underbrace{g\tan\alpha}_{\text{resistance}} \tag{1}$$

Eq. (1), also known as West's formula (Milne 1885; Kirkpatrick 1927), shows that the block $<b, h>$ will uplift when $\ddot{u}_g \geq g\tan\alpha$. Now, given that this is a *quasi-static* lateral inertial loading, the inertia moment due to the nearly zero rotational accelerations of the blocks is negligible $[\ddot{\theta}(t) = 0]$. Once uplift has occurred, the rocking block experiences a positive rotation, $\theta(t)$; therefore, the seismic demand is $m\ddot{u}_g R\cos[\alpha - \theta(t)]$, whereas the seismic resistance is merely $mgR\sin[\alpha - \theta(t)]$ because $\ddot{\theta}(t) = 0$. For $\theta > 0$, the resistance of the rocking block upon uplifting under quasi-static lateral loading is $\tan[\alpha - \theta(t)]$, which is smaller than $\tan\alpha$. Accordingly, once the block uplifts, it will also overturn. From this analysis, one concludes that, under quasi-static lateral loading, the stability of a free-standing column depends solely on its slenderness ($g\tan\alpha$) and is independent of the size ($R = \sqrt{b^2 + h^2}$).

Seismic Resistance of Free-Standing Columns Subjected to Dynamic Loads

In reality, earthquake shaking, $\ddot{u}_g$, is not a quasi-static loading, and once uplifting has occurred, the block will experience a finite rotational acceleration $[\ddot{\theta}(t) \neq 0]$. In this case, dynamic moment equilibrium gives

$$\underbrace{-m\ddot{u}_g(t)R\cos[\alpha - \theta(t)]}_{\text{seismic demand}} = \underbrace{I_o\ddot{\theta}(t) + mgR\sin[\alpha - \theta(t)]}_{\text{seismic resistance}}, \qquad \theta > 0 \tag{2}$$

where I_o = the rotational moment of inertia of the column about the pivot point at the base—a quantity that is proportional to the square of the size of the column, R. As an example for rectangular columns, $I_o = (4/3)\,mR^2$, and Eq. (2) simplifies to

$$\underbrace{-\ddot{u}_g(t)R\cos[\alpha - \theta(t)]}_{\text{seismic demand}} = \underbrace{\frac{4}{3}R^2\ddot{\theta}(t) + gR\sin[\alpha - \theta(t)]}_{\text{seismic resistance}}, \qquad \theta > 0 \tag{3}$$

Eq. (3) indicates that when a slender free-standing column is set into rocking motion, the seismic demand (overturning seismic moment) is proportional to R (first power of the size), whereas the seismic resistance (opposition to rocking) is proportional to R^2 (second power of the size). Consequently, Eq. (3) dictates that, for a given ground motion, regardless of how slender a column is (small α) and how intense the ground shaking, $\ddot{u}_g$, is (large seismic demand), when a rotating column [$\ddot{\theta}(t)$ = finite] is large enough, the second power of R on the right-hand side (seismic resistance) can always ensure stability. Simply stated, Housner's (1963) size-frequency effect is merely a reminder that a quadratic term eventually dominates over a linear term, regardless of the values of their individual coefficients.

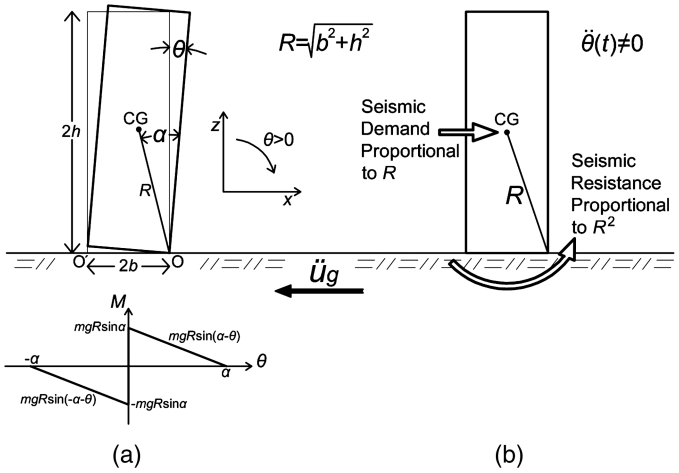

Fig. 1. (a) Geometric characteristics of a free-standing rocking column together with its moment rotation diagram; (b) during earthquake shaking that sets the column in rocking motion $[\theta(t) \neq 0]$, the seismic resistance is proportional to R^2, whereas the seismic demand is proportional to R; consequently, when a free-standing column is sufficiently large, it can survive large horizontal accelerations even if it is very slender

Fig. 1(b) schematically shows the relations with size R of the seismic demand (linear relation) and the seismic resistance (quadratic relation). From its very conception the "equivalent static lateral force analysis" is not meant to deal with any rotational acceleration term; a fact that leads to its notable failure to capture the seismic stability (resistance) of tall free-standing structures.

When a column is vertically restrained with a tendon that passes along its centerline, as shown in Fig. 2, the restoring moment of the tendon is also proportional to the first power of the width of the column. Accordingly, as the size of the column increases, the seismic resistance that originates from the difficulty to mobilize the rotational inertia of the column increases with R^2, and eventually it will dominate over the resistance from the tendon (proportional to $R\sin\alpha$)—even if the tendon is very stiff—as is shown in this paper.

Dynamics of a Rocking Column with a Vertical Restrainer along Its Centerline

This section examines the dynamics of the solitary rocking column with a vertical elastic restrainer along its centerline, as shown in Fig. 2(a). Following Housner's (1963) approach, both the column and the underlying soil are assumed to be rigid. For rocking on deformable support, the reader is referred to Chatzis and Smyth (2011), and for rocking of flexible bodies, the reader is referred to Acikgoz and DeJong (2012) and Vassiliou et al. (2014). This assumption would represent a relatively stiff column rocking on a rigid foundation. When the elasticity, EA, of the restrainer is small compared to the weight of the rocking columns, $m_c g$, the lateral stiffness of the systems remains negative upon uplifting, as is in the free rocking case. As the elasticity, EA, of the restrainer

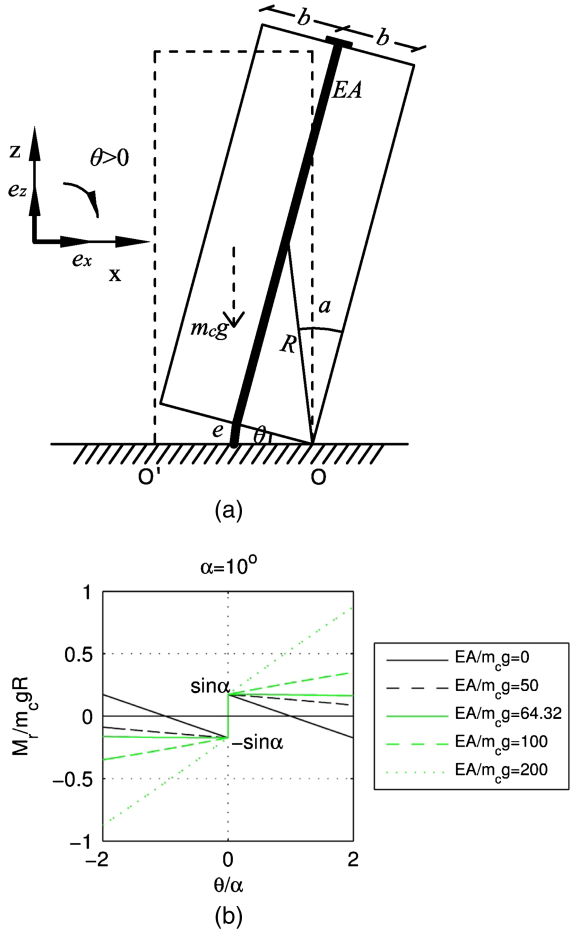

Fig. 2. (a) Vertically restrained rocking column with slenderness $\tan\alpha = b/h$ and size $R = \sqrt{b^2 + h^2}$ (b) and its moment rotation diagram for various values of the dimensionless stiffness of the tendon $EA/m_c g$

increases, the lateral stiffness of the vertical rocking column increases gradually from negative to positive, as shown in Fig. 2(b). Depending on the characteristics of the column, a linear spring could be connected in series so that the system remains elastic for the expected range of rotations (Cheng 2008). In that case, the term $EA/2h$ in the following equations should be replaced by the equivalent stiffness of the spring-tendon system.

Assuming that the rocking column will not topple, it will recenter, impact will happen at the new pivot point, and subsequently it will rock with opposite rotations. During rocking, the horizontal and vertical displacement of the center of mass, $u(t)$ and $v(t)$, are given for $\theta(t) < 0$ and $\theta(t) > 0$ by the following expressions:

$$u(t) = \mp R[\sin\alpha - \sin(\alpha \pm \theta)] \tag{4}$$

$$v(t) = R[\cos(\alpha \pm \theta) - \cos\alpha] \tag{5}$$

In Eqs. (4) and (5), whenever there is a double sign (such as $\mp$), the top sign is for $\theta < 0$ and the bottom sign is for $\theta > 0$.

Regardless of the sign of the rotation $\theta(t)$, during an admissible rotation, $\delta\theta$, the variations of the work, δW, done by the external field forces is

$$\delta W = -m_c(\ddot{u}_g \delta u + g\delta v) \tag{6}$$

Case 1 $\theta(t) > 0$

During this admissible rotation $\delta\theta$, the variation of the work, δW, and the variations of the displacements δu and δv are

$$\delta u = \frac{du}{d\theta}\delta\theta \tag{7}$$

$$\text{and } \delta v = \frac{dv}{d\theta}\delta\theta \tag{8}$$

After differentiating Eqs. (4) and (5) for $\theta > 0$ with respect to θ, Eqs. (7) and (8) give

$$\delta u = R\cos(\alpha - \theta)\delta\theta \tag{9}$$

$$\delta v = R\sin(\alpha - \theta)\delta\theta \tag{10}$$

Substitution of Eqs. (9) and (10) into Eq. (6) gives

$$\frac{dW}{d\theta} = -m_c R[\ddot{u}_g \cos(\alpha - \theta) + g\sin(\alpha - \theta)], \qquad \theta > 0 \tag{11}$$

During rocking motion of the vertically restrained column, in addition to the work of the external field forces, W, work is done by the axial force in the tendon, $P = (EA/2h)\,e$, where e is the elongation of the tendon due to the rocking motion. With reference to Fig. 2(a):

$$e = R\sin\alpha\sqrt{2}\sqrt{(1 - \cos\theta)} \tag{12}$$

In addition to the elongation, e, this analysis includes an initial elongation, e_o, in the tendon due to a possible initial post-tensioning, $P_o = (EA/2h)\,e_o$. Accordingly, regardless of the sign of the rotation $\theta(t)$, the potential energy due to the axial force along the tendon is

$$V = \frac{1}{2}\frac{EA}{2R\cos\alpha}(e + e_o)^2 \tag{13}$$

In the previous equation, it is assumed that the tendon force is constant along its length.

Substituting Eq. (12) into (13), and after differentiation with respect to the independent variable, θ, one obtains

$$\frac{dV}{d\theta} = R\sin\alpha\sin\theta\left(\frac{EA}{2\cos\alpha}\sin\alpha + \frac{Po}{\sqrt{2 - 2\cos\theta}}\right) \tag{14}$$

During rocking motion, Lagrange's equation shall be satisfied:

$$\frac{d}{dt}\left[\frac{d(T - V)}{d\dot{\theta}}\right] - \frac{d(T - V)}{d\theta} = \frac{dW}{d\theta} \tag{15}$$

where T = the relative-to-the-ground kinetic energy of the system, whereas $dW/d\theta$ and $dV/d\theta$ are given by Eqs. (11) and (14), respectively.

In either case where $\theta(t) < 0$ or $\theta(t) > 0$, the kinetic energy of the system is

$$T = \frac{1}{2}I_o\dot{\theta}^2(t) \tag{16}$$

The substitution of Eqs. (11), (14), and (16) into Lagrange's Eq. (15) results in the equation of motion of the rocking column with a vertical restrainer along its centerline for $\theta(t) > 0$:

$$I_o\ddot{\theta}(t) = -m_c R[\ddot{u}_g \cos(\alpha-\theta) + g\sin(\alpha-\theta)] - R\sin\alpha\sin\theta\left[\frac{1}{2}EA\tan\alpha + \frac{P_o}{\sqrt{2}\sqrt{(1-\cos\theta)}}\right] \quad (17)$$

Eq. (17) further simplifies to

$$\ddot{\theta}(t) = -p^2\left\{\sin(\alpha-\theta) + \frac{\ddot{u}_g}{g}\cos(\alpha-\theta) + \sin\alpha\sin\theta\left[\frac{1}{2}\frac{EA}{m_c g}\tan\alpha + \frac{F_o}{m_c g}\frac{1}{\sqrt{2}\sqrt{(1-\cos\theta)}}\right]\right\} \quad (18)$$

where $p = \sqrt{m_c R g/I_o}$ = the frequency parameter of the column. For a rectangular column, $I_o = (4/3)m_c R^2$ and the frequency parameter assumes the value $p = \sqrt{3g/4R}$.

Similar derivations for $\theta < 0$ lead to a single equation:

$$\ddot{\theta}(t) = -p^2\left\{\sin(\alpha\text{sgn}\theta - \theta) + \frac{\ddot{u}_g}{g}\cos(\alpha\text{sgn}\theta - \theta) + \sin\alpha\sin\theta\left[\frac{1}{2}\frac{EA}{m_c g}\tan\alpha + \frac{P_o}{m_c g}\frac{1}{\sqrt{2}\sqrt{(1-\cos\theta)}}\right] \text{ elasticity prestressing}\right\} \quad (19)$$

which is identical to the *preyield* expression (without prestress) given in Dimitrakopoulos and DeJong (2012). However, unlike the approach used by Dimitrakopoulos and DeJong, the restraining mechanism in this case is assumed to behave elastically. An approximate expression of Eq. (19) has been presented by Barthes et al. (2010).

During the oscillatory rocking motion of the vertically restrained rigid column, the moment-rotation behavior that depends on the elasticity of the tendon and the level of prestressing is expressed with one of the curves shown in Fig. 2(b) without enclosing any area. Energy is lost only during impact when the angle of rotation reverses. At this instant, it is assumed that the rotation continues smoothly from points O to O′, and that the impact force is concentrated at the new pivot point. With this idealization, the impact force does not apply any moment about the new pivot point O′, hence the new impact force does not influence the moment of momentum of the rocking column after the impact. Similarly, during impact $[\theta(t) = 0]$, the elongation of the tendon, e, given by Eq. (12) is zero, whereas any finite force due to prestressing shall be the same prior to and after the impact. Accordingly, any forces in the tendon at the instant of impact do not create any change in the moment of momentum prior to and after the impact. Following this reasoning, the ratio of the kinetic energy after and before the impact is offered by the same expression derived from the conservation of the moment of momentum of the free-standing column:

$$r = \frac{\dot{\theta}_2^2}{\dot{\theta}_1^2} = \left(1 - \frac{3}{2}\sin^2\alpha\right)^2 \quad (20)$$

This reasoning has been used to address the dynamics of more complex configurations (Vassiliou and Makris 2012).

From Negative to Positive Stiffness

In the vertically restrained rocking column, the negative stiffness originates from the fact that as rotation increases, the restoring weight vector of the column approaches the pivot point, whereas the positive stiffness originates from the presence of the vertical elastic restrainer, which offers an increasing restoring moment.

Without loss of generality, this study concentrates on the case of positive rotations $[\theta(t) > 0]$. Eq. (17) indicates that the rotation-dependent restoring moment is

$$M_r(\theta) = m_c g R\left[\sin(\alpha-\theta) + \sin\alpha\sin\theta\left(\frac{\tan a}{2}\frac{EA}{m_c g} + \frac{P_o}{m_c g}\frac{1}{\sqrt{2}\sqrt{1-\cos\theta}}\right)\right] \quad (21)$$

which after rearranging terms assumes the form

$$\frac{M_r(\theta)}{m_c g R} = \sin\alpha\left[\cos\theta + \sin\theta\left(\frac{P_o}{m_c g\sqrt{2}}\frac{1}{\sqrt{1-\cos\theta}} + \frac{1}{2}\tan\alpha\frac{EA}{m_c g} - \cot\alpha\right)\right] \quad (22)$$

Fig. 2(b) plots the expression given by Eq. (22) for various values of the dimensionless elastic force, $EA/m_c g$, for a column with slenderness $\alpha = 10°$ and for $P_o/m_c g = 0$. Furthermore, Fig. 2(b) reveals that, whereas the right-hand side of Eq. (22) is nonlinear, the restoring moment exhibits a nearly linear dependence on the rotation, θ. When linearizing Eq. (22) $[1-\cos\theta \approx \theta^2)/2$, $\sin\theta \approx \theta\cos\theta \approx 1]$:

$$\frac{M_r(\theta)}{m_c g R} = \sin\alpha\left[1 + \frac{P_o}{m_c g} + \theta\left(\frac{1}{2}\tan\alpha\frac{EA}{m_c g} - \cot\alpha\right)\right] \quad (23)$$

Clearly, Fig. 2(b) and Eq. (23) show that as the elasticity of the tendon increases, the initial slope of the restoring moment goes from negative to positive. The factor of the rotation θ in Eq. (23) is the stiffness of the system upon uplifting, and therefore, the condition for the linearized system to exhibit a positive stiffness is

$$\frac{EA}{m_c g} > 2\frac{1}{\tan^2\alpha} \quad (24)$$

For instance, according to expression (24), a vertically rocking column exhibits a positive stiffness when $(EA/m_c g) > 64.32$ for $\alpha = 10°$ and when $(EA/m_c g) > 32.17$ for $\alpha = 14°$. When expression (24) becomes an equality, the vertically restrained rocking column exhibits a rigid-plastic behavior, as shown in Fig. 2(b). It can be confirmed that the linearization of the system as presented by Eq. (23) offers dependable results, even for values of the rotation θ as large as the slenderness α. As an example, when one works with the nonlinear expression given by Eq. (22) (Vassiliou 2010), the exact value of $EA/m_c g$ that keeps the derivative $dM_r(\theta)/d(\theta)$ positive is

$$\frac{EA}{m_c g} > 2\frac{1+\tan^2\alpha}{\tan^2\alpha} \quad (25)$$

The difference between inequalities (24) and (25) is 3.0% when $\alpha = 10°$ and 6.0% when $\alpha = 14°$.

Rocking Spectra of the Vertically Restrained Solitary Column: Self-Similar Response

The various mathematical idealizations of coherent pulse-type ground motions as described in several publications over the last half century (Veletsos and Newmark 1960; Veletsos et al. 1965; Bertero et al. 1978; Hall et al. 1995; Makris 1997; Makris and Chang 2000; Alavi and Krawinkler 2001; Mavroeidis and Papageorgiou 2003, Makris and Psychogios 2006; Baker 2007;

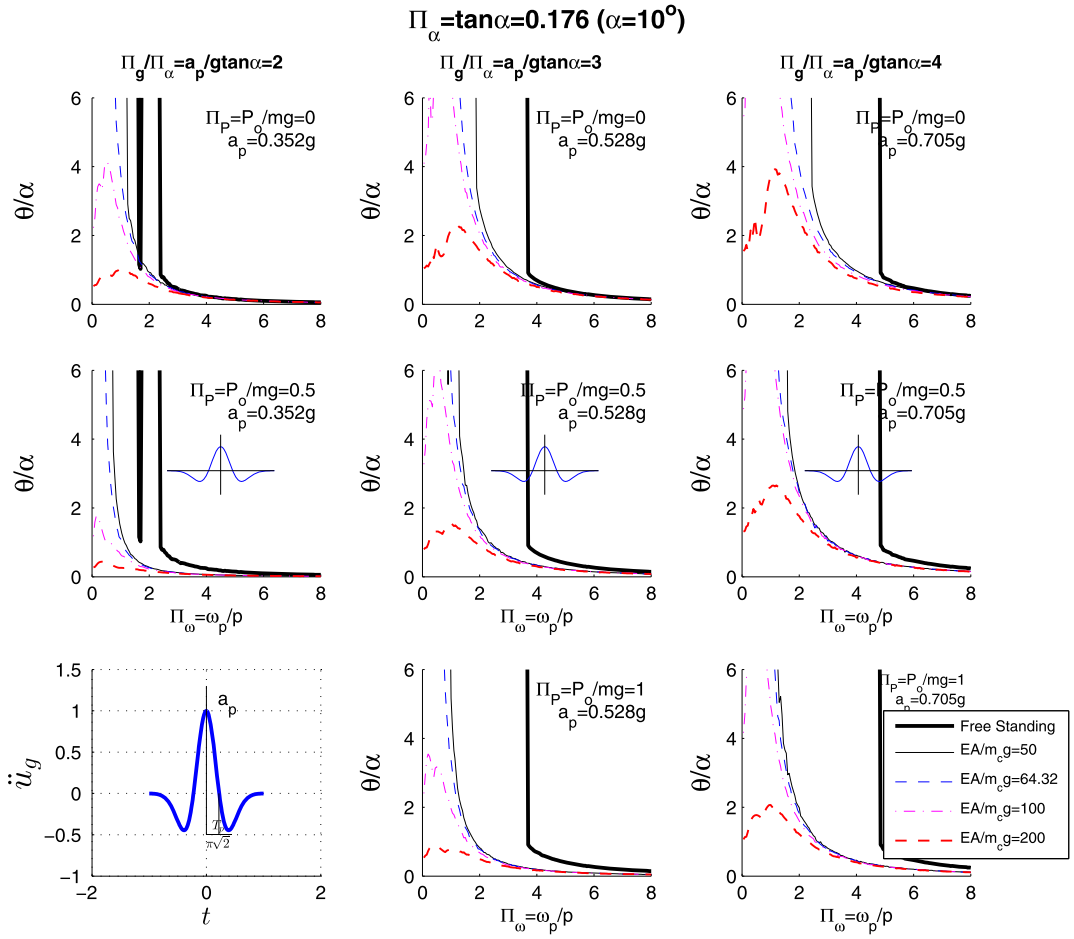

Fig. 3. Rocking spectra for different values of the dimensionless products, $\Pi_g = a_p/g$, $\Pi_E = EA/m_c g$, and $\Pi_p = P_o/m_c g$, when the solitary rocking column with slenderness $\alpha = 10°$ ($\Pi_\alpha = \tan\alpha = 0.176$) is subjected to a symmetric Ricker wavelet; for values of $\Pi_\omega = \omega_p/p > 5$, the response of the free-standing column is essentially identical to the response of the restrained column

Vassiliou and Makris 2011, among others) are invariably characterized by a pulse period, T_p, and a pulse acceleration amplitude, a_p.

The current established methodologies for estimating the pulse characteristics of a wide class of records are of unique value, because the product, $a_p T_p^2 = L_p$, is a characteristic length scale of the ground excitation and is a measure of the persistence of the most energetic pulse to generate inelastic deformation (Makris and Black 2004a, b; Karavasilis et al. 2010). It is emphasized that the persistence of the pulse, $a_p T_p^2 = L_p$, is a different characteristic than the strength of the pulse, which is measured with the peak pulse acceleration, a_p. The reader may recall that among two pulses with different acceleration amplitudes (such as $a_{p1} > a_{p2}$) and different pulse durations (such as $T_{p1} < T_{p2}$), the inelastic deformation does not scale with the peak pulse acceleration (most intense pulse) but with the strongest length scale (larger $a_p T_p^2$ = most persistent pulse) (Makris and Black 2004a, b; Karavasilis et al. 2010).

The heavy dark line in Fig. 3 (bottom left) is a scaled expression of the second derivative of the Gaussian distribution, $e^{-t^2/2}$, known in the seismological literature as the symmetric Ricker wavelet (Ricker 1943, 1944):

$$\psi(t) = a_p\left(1 - \frac{2\pi^2 t^2}{T_p^2}\right) e^{-\frac{12\pi^2 t^2}{2\ T_p^2}} \tag{26}$$

The wavelet given by Eq. (26) or its time derivative can satisfactorily approximate the coherent pulse of several pulse-like ground motions (Gazetas et al. 2009; Vassiliou and Makris 2011). The value of $T_p = 2\pi/\omega_p$ is the period that maximizes the Fourier spectrum of the symmetric Ricker wavelet.

The choice of the specific functional expression to approximate the main pulse of pulse-type ground motions has limited significance in this work. What is important to recognize is that several strong ground motions contain a distinguishable acceleration pulse that is responsible for most of the inelastic deformation of structures (Hall et al. 1995; Makris and Chang 2000; Alavi and Krawinkler 2001; Makris and Black 2004a, b; Makris and Psychogios 2006, among others). A mathematically rigorous and easily reproducible methodology based on wavelet analysis to construct the best matching wavelet has been recently proposed by Vassiliou and Makris (2011).

The first two terms on the right-hand side of Eq. (19) express the response of the solitary free-standing column, which is fully described by four independent dimensionless variables (Makris and Vassiliou 2013): $\Pi_\theta = \theta$, $\Pi_\omega = \omega_p/p$, $\Pi_a = \tan\alpha$, and $\Pi_g = a_p/g$, where a_p and $\omega_p = 2\pi/T_p$ are the acceleration amplitude and the cyclic frequency of the excitation pulse.

The contributions of the elasticity, E, and the prestressing force of the tendon, P_o, are entered into Eq. (19) in a dimensionless form, $\Pi_E = EA/m_c g$ and $\Pi_P = P_o/m_c g$.

With the six dimensionless Π terms established, the dynamic response of the vertically restrained solitary column can be expressed as a function of six nondimensional variables:

$$\theta(t) = \varphi\left(\frac{\omega_p}{p}, \tan\alpha, \frac{a_p}{g}, \frac{EA}{m_c g}, \frac{P_o}{m_c g}, pt\right) \tag{27}$$

Contingency of Resonance

Eq. (23) indicates that the linearized rotational stiffness of the vertically restrained rocking column is given by

$$K_r = m_c g R \sin\alpha\left(\frac{1}{2}\tan\alpha\frac{EA}{m_c g} - \frac{1}{\tan\alpha}\right) \tag{28}$$

When $EA/m_c g$ is sufficiently large and satisfies inequality (24), K_r is positive, and upon uplifting ($\theta \neq 0$), the rotational frequency of the system is

$$\omega_r^2 = \frac{m_c g R \sin\alpha\left(\frac{1}{2}\tan\alpha\frac{EA}{m_c g} - \frac{1}{\tan\alpha}\right)}{I_o} \tag{29}$$

The rocking system is not a linear system. It follows a bilinear law and it dissipates energy at each impact. Hence, in a strict sense, it does not have a frequency. However, it has been shown (Makris and Kampas 2013) that a term similar to the one offered by Eq. (29) is a meaningful quantity that can be used as a frequency to predict quasi-resonance effects.

Recognizing that $p^2 = m_c g R/I_o$ and that, for slender columns, $\sin\alpha \approx \tan\alpha$, Eq. (29) gives

$$\omega_r = p\sqrt{\frac{1}{2}\tan^2\alpha\frac{EA}{m_c g} - 1} \tag{30}$$

At resonance, $\omega_p = \omega_r$, and this happens when

$$\frac{\omega_p}{p} = \sqrt{\frac{1}{2}\tan^2\alpha\frac{EA}{m_c g} - 1} \tag{31}$$

or in terms of dimensionless products, the vertically restrained rocking columns are at resonance when

$$\Pi_\omega = \sqrt{\frac{1}{2}\Pi_\alpha^2\Pi_E - 1} \tag{32}$$

For instance, according to Eq. (32), when $\alpha = 10°$ and $(EA/m_c g) = 100 > 64.33$, the system is at resonance when $\omega_p/p = 0.75$, whereas when $EA/m_c g = 200$, the system is at resonance when $\omega_p/p = 1.45$. Eq. (32) is expected to give a better approximation of the resonance frequency when the system moves more along the post-uplift branch of the M-θ curve.

Interpretation of the Dynamic Response

Fig. 3 shows rocking spectra for different values of the dimensionless products Π_g, Π_E, and Π_P when the solitary column with

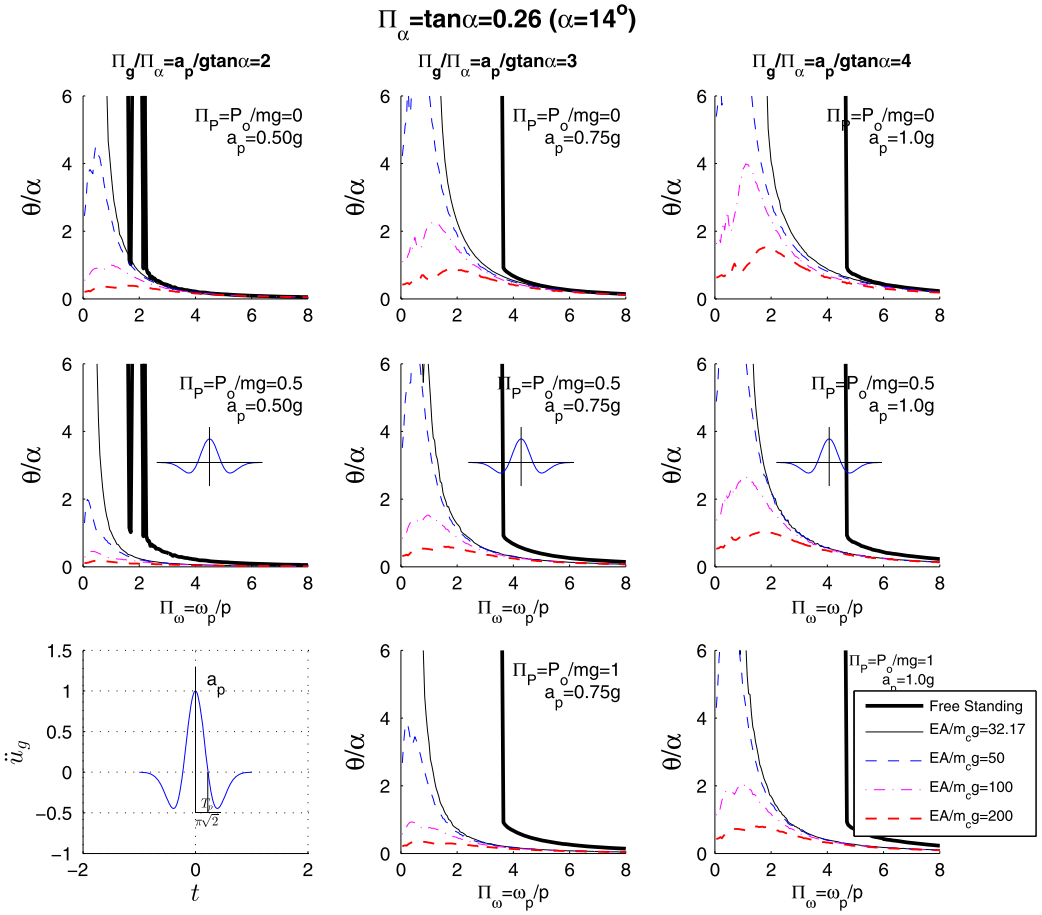

Fig. 4. Rocking spectra for different values of the dimensionless products, $\Pi_g = a_p/g$, $\Pi_E = EA/m_c g$, and $\Pi_p = P_o/m_c g$, when the solitary rocking column with slenderness $\alpha = 14°$ ($\Pi_\alpha = \tan\alpha = 0.26$) is subjected to a symmetric Ricker wavelet; for values of $\Pi_\omega = \omega_p/p > 5$, the response of the free-standing column is essentially identical to the response of the restrained column

slenderness $\alpha = 10°(\Pi_\alpha = \tan\alpha = 0.176)$ is subjected to a symmetric Ricker pulse (Mexican hat).

When a free-standing column with slenderness α is subjected to a horizontal ground acceleration, with peak value a_p, the column uplifts only when $a_p > g\tan\alpha$. In the case where a vertical tendon is present, at the initiation of motion $[\theta(t) = 0]$, the tendon will exert a finite restoring moment only if it is prestressed $(P_o \neq 0)$. In this case, moment equilibrium about the imminent pivot point gives the minimum uplift acceleration:

$$\ddot{u}_g^{\text{up}} = g\tan\alpha\left(1 + \frac{P_o}{m_c g}\right) \tag{33}$$

Accordingly, rocking will take place only when $\Pi_g/\Pi_\alpha = (a_p/g\tan\alpha) > 1 + (P_o/m_c g) = 1 + \Pi_p$.

The left plots in Fig. 3 are for $a_p = 0.352$ g $(\Pi_g/\Pi_a = a_p/g\tan\alpha = 2)$ and the center plots are for $a_p = 0.528$ g $(\Pi_g/\Pi_a = 3)$, whereas the right plots are for $a_p = 0.705$ g $(\Pi_g/\Pi_a = 4)$. All plots show that, at small values of ω_p/p (small columns or long duration pulses), the free-standing columns overturn, whereas the restrained columns with positive stiffness $[\Pi_E = (EA/mg) > 2/(\tan^2\alpha)]$ exhibit the expected amplification in the neighborhood of resonance $[\Pi_\omega = \omega_p/p = \sqrt{(1/2)\Pi_\alpha^2\Pi_E - 1}]$. On the other hand, as ω_p/p increases, the responses from all configurations reduce to a single curve, showing that the effect of the vertical tendons is marginal compared to the seismic resistance that originates from the mobilization of the rotational inertia of the column.

At this point, it is worth translating the dimensionless products of Fig. 3 to physical quantities of typical bridges. First, a 9.6-m-tall pier with width $2b = 1.6$ m$(R = 4.87$ m, $p = 1.23$ rad/s, and $\tan\alpha = 1.6/9.6$ m $= 0.166)$ is considered. These are typical dimensions of bridge piers of highway overpasses and other smaller bridges in Europe and the United States (Zhang et al. 2004; Makris and Zhang 2004). With reference to Fig. 3, the 9.6×1.6 m free-standing column is excited by the Ricker pulse that approximates the strong 1992 Erzincan, Turkey record ($a_p = 0.35$ g, $T_p = 1.44$ s). This gives $\Pi_\omega = \omega_p/p = 2\pi/pT_p = 3.54$. Fig. 3 (left) that is plotted for a given value of $a_p = 0.352$ g, shows that at $\omega_p/p = 3.54$, the effect of the restrainers is marginal and that the free-standing column experiences approximately the same uplift as the column with a restrainer with $EA = 200m_c g$. Fig. 3 (center) indicates that if the acceleration amplitude of the 1.44-s-long Ricker pulse is increased to $a_p = 0.53$ g, the 9.6×1.6 m

Table 1. Earthquake Records Used for the Seismic Response Analysis of the Free-Standing Rocking Bridge Bent

Earthquake	Record	Magnitude (Mw)	Epicentral distance (km)	PGA (g)	PGV (m/s)	a_p (g)	T_p (s)
1966 Parkfield	CO2/065	6.1	0.1	0.48	0.75	0.41	0.6
1971 San Fernando	Pacoima Dam/164	6.6	11.9	1.23	1.13	0.38	1.27
1986 San Salvador	Geotech Investigation Center	5.4	4.3	0.48	0.48	0.34	0.8
1992 Erzincan	Erzincan/EW	6.9	13	0.50	0.64	0.34	0.9
1994 Northridge	Jensen Filter Plant/022	6.7	6.2	0.57	0.76	0.39	0.5
1995 Kobe	Takarazuka/000	6.9	1.2	0.69	0.69	0.50	1.1

Note: PGA = peak ground acceleration; PGV = peak ground velocity.

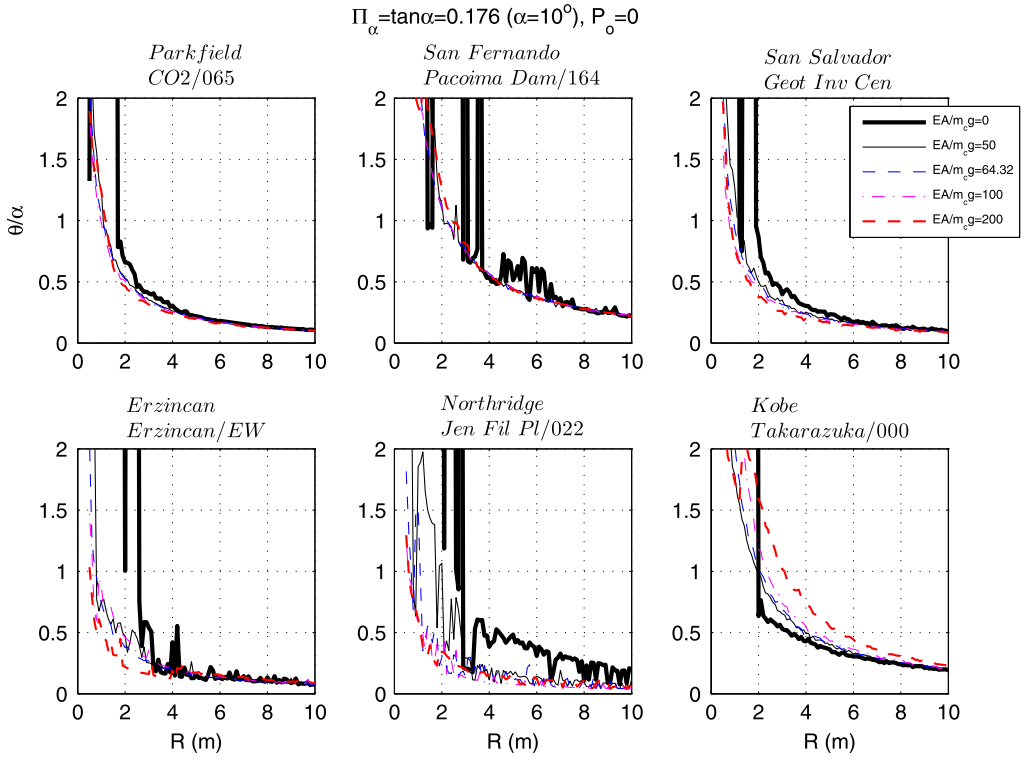

Fig. 5. Rocking spectra (peak uplift rotation) of vertically restrained columns with slenderness $\alpha = 10°$, various values of the elasticity of the tendon $(\Pi_E = EA/m_c g)$, and zero prestressing $(\Pi_p = P_o/m_c g = 0)$

free-standing column overturns; however, its stability is appreciably enhanced even with the use of a flexible tendon ($EA/m_c g = 50$), which maintains a negative stiffness.

A 24-m-tall bridge pier with width $2b = 4.0$ m($R = 12.17$ m, $p = 0.778$, and $\tan\alpha = 4/24 = 0.166$) is now considered. Such tall piers are common in valley bridges (Makris et al. 2010). It is assumed that the 24×4 m free-standing pier is excited by the Ricker pulse shown in Fig. 3 with $a_p = 0.35$ g and $T_p = 1.44$ s. This gives $\Pi_\omega = \omega_p/p = 2\pi/pT_p = 5.61$. For such a large value of ω_p/p, the 24×4 m free-standing pier survives the 1.44 s long acceleration pulse, even when its acceleration amplitude is as high as $a_p = 0.705$ g. The main conclusion is that as the size of the column increases or the frequency of the pulse increases, the effect of vertical tendons becomes immaterial given that most of the seismic resistance originates from the mobilization of the rotational inertia of the column.

Fig. 4 shows rocking spectra for different values of the dimensionless products Π_g, Π_E, and Π_P when a more squat solitary column (slenderness $\alpha = 14°$; $\Pi_\alpha = \tan\alpha = 0.26$) is subjected to a symmetric Ricker pulse (Mexican hat). The results are qualitatively similar to the case of the more slender ($\alpha = 10°$) column.

The seismic response analysis of the vertically restrained solitary column has been studied in this section by using acceleration pulses as ground excitation. The acceleration amplitude, a_p, and the duration, T_p, of any acceleration wavelet allow the use of the dimensional analysis presented in this work and the derivation of the associated Π products, which improve the understanding of the physics that govern the problem together with the organization and presentation of the response. The response analysis proceeds by producing rocking spectra of vertically restrained columns when subjected to six strong-motion historic records listed in Table 1. The values of the acceleration amplitudes, a_p, and pulse periods, T_p, shown in the last two columns of Table 1 have been determined with the extended wavelet transform (Vassiliou and Makris 2011).

Fig. 5 plots rocking spectra (peak uplift rotation) of vertically restrained columns with slenderness $\alpha = 10°$ as their size R increases. The reader is reminded that the size R of the columns is related to the frequency parameter of the column,

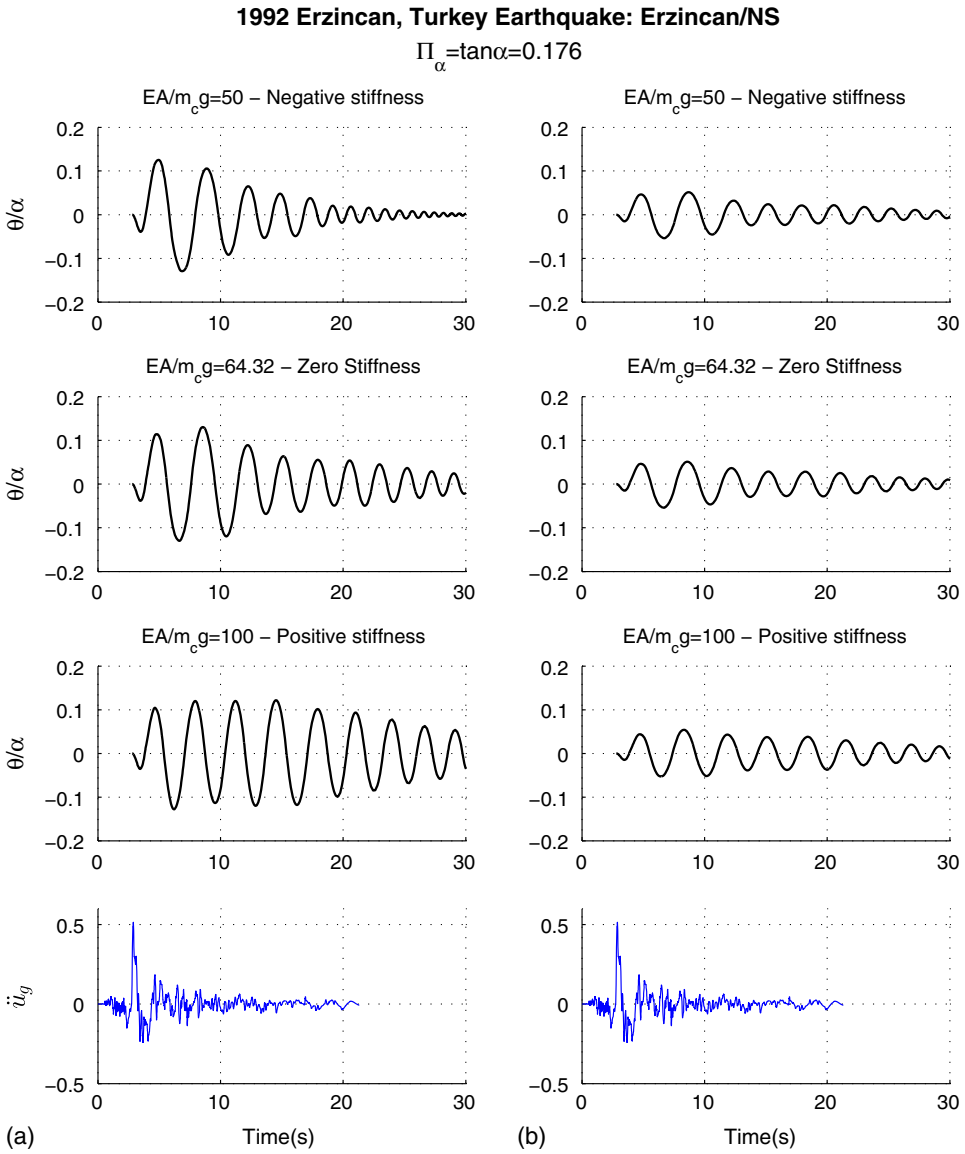

Fig. 6. Rotation response histories of a 9.6-m-tall column (a) and a 24-m-tall column (b) when subjected to the 1992 Erzincan, Turkey earthquake record; both columns have slenderness $\alpha = 10°$; peak rotation of both columns is essentially independent of the stiffness of the restrainer

$p = \sqrt{m_c g R / I_o}$. The columns are subjected to the six strong earthquake records listed in Table 1. Fig. 5 indicates that when the size $R = \sqrt{b^2 + h^2}$ of the columns is larger than 5 m, their uplift response is essentially independent of whether the column is free standing or restrained with a tendon that is as stiff as $EA = 200 m_c g$. The other important information offered by Fig. 5 is that a free-standing column as slender as $\alpha = 10°(\tan\alpha = 0.167)$ survives any of the six strong motions listed in Table 1 when its size R is larger than 4.0 m ($R > 4$ m). Furthermore, Fig. 5 shows that for medium-size columns ($4 < R < 6$ m), a relative flexible tendon that maintains a negative stiffness in the system offers a seismic response comparable to stiffer tendons that induce unnecessary high stresses into the system at the pivot points both during the rocking phase and during the impact.

Fig. 6 plots the rotation response histories of a 9.6-m-tall column and a 24-m-tall column when subjected to the 1992 Erzincan, Turkey earthquake record. The slenderness of both columns is $\alpha = 10°$. Fig. 6 indicates that when the stiffness of the tendon increases, the decay of the system response is more feeble due to the energy that is stored in the tendon.

Conclusions

This paper investigated the rocking response of a slender column that is vertically restrained with an elastic tendon that passes through its centerline.

Whereas the stiffness of a free-standing column is negative, the stiffness of a vertically restrained column can be anywhere from negative to positive, depending on the stiffness of the tendon. Following a variational formulation, the paper shows that vertical tendons are effective in suppressing the response of smaller columns subjected to long-period excitations. As the size of the column or the frequency of the excitation increases, the effect of the vertical tendon becomes increasingly immaterial given that most of the seismic resistance of large rocking columns originates primarily from the mobilization of the rotational inertia of the column. The paper shows that, for medium-size rocking columns where the concept of vertical restrainers may be attractive, there is a merit for the vertical tendons to be flexible enough so that the overall lateral stiffness of the system remains negative. In this way, the pivot points are not overloaded with high compressive forces, while at the same time the rocking structure enjoys ample seismic stability.

Acknowledgments

This work was funded by the research project Seismo-Rock Bridge with Grant No. 2295, which is implemented under the ARISTEIA action of the Operational Programme Education and Lifelong Learning, and was cofunded by the European Social Fund (ESF) and Greek National Resources.

References

Acikgoz, S., and DeJong, M. J. (2012). "The interaction of elasticity and rocking in flexible structures allowed to uplift." *Earthquake Eng. Struct. Dyn.*, 41(15), 2177–2194.

Alavi, B., and Krawinkler, H. (2001). "Effects of near-source ground motions on frame-structures." *Technical Rep. No. 138*, The John A. Blume Earthquake Engineering Center, Stanford University, Stanford, CA.

Baker, J. W. (2007). "Quantitative classification of near-fault ground motions using wavelet analysis." *Bull. Seismol. Soc. Am.*, 97(5), 1486–1501.

Barthes, C., Hube, M, and Stojadinovic, B. (2010). "Dynamics of a post-tensioned rocking block." *Proc., 9th U.S. National and 10th Canadian Conf. on Earthquake Engineering*, Toronto, Canada.

Bertero, V. V., Mahin, S. A., and Herrera, R. A. (1978). "Aseismic design implications of near-fault san fernando earthquake records." *Earthquake Eng. Struct. Dyn.*, 6(1), 31–42.

Chatzis, M. N., and Smyth, A. W. (2011). "Robust modeling of the rocking problem." *J. Eng. Mech.*, 10.1061/(ASCE)EM.1943-7889.0000329. 247–262.

Cheng, C. T. (2007). "Energy dissipation in rocking bridge piers under free vibration tests." *Earthquake Eng. Struct. Dyn.*, 36(4), 503–518.

Cheng, C. T. (2008). "Shaking table tests of a self-centering designed bridge substructure." *Eng. Struct.*, 30(12), 3426–3433.

Christopoulos, C., Filiatrault, A., Uang, C. M., and Folz, B. (2002). "Post-tensioned energy dissipating connections for moment-resisting steel frames." *J. Struct. Eng.*, 10.1061/(ASCE)0733-9445(2002)128:9(1111), 1111–1120.

Cohagen, L., Pang, J. B. K., Stanton, J. F., and Eberhard, M. O. (2008). "A precast concrete bridge bent designed to recenter after an earthquake." *Research Rep.*, Federal Highway Administration, Washington, DC.

Dimitrakopoulos, E. G., and DeJong, M. J. (2012). "Overturning of retrofitted rocking structures under pulse-type excitations." *J. Eng. Mech.*, 10.1061/(ASCE)EM.1943-7889.0000410., 963–972.

Gazetas, G., Garini, E., Anastasopoulos, I., and Georgarakos, T. (2009). "Effects of near-fault ground shaking on sliding systems." *J. Geotech. Geoenviron. Eng.*, 10.1061/(ASCE)GT.1943-5606.0000174., 1906–1921.

Hall, J. F., Heaton, T. H., Halling, M. W., and Wald, D. J. (1995). "Near-source ground motion and its effects on flexible buildings." *Earthquake Spectra*, 11(4), 569–605.

Housner, G. W. (1963). "The behavior of inverted pendulum structures during earthquakes." *Bull. Seismol. Soc. Am.*, 53(2), 403–417.

Kam, W. Y., Pampanin, S., Palermo, A., and Carr, A. J. (2010). "Self-centering structural systems with combination of hysteretic and viscous energy dissipations." *Earthquake Eng. Struct. Dyn.*, 39(10), 1083–1108.

Karavasilis, T. L., Makris, N., Bazeos, N., and Beskos, D. E. (2010). "Dimensional response analysis of multistory regular steel MRF subjected to pulselike earthquake ground motions." *J. Struct. Eng.*, 10.1061/(ASCE)ST.1943-541X.0000193, 921–932.

Kirkpatrick, P. (1927). "Seismic measurements by the overthrow of columns." *Bull. Seismol. Soc. Am.*, 17(2), 95–109.

Mahin, S., Sakai, J., and Jeong, H. (2006). "Use of partially prestressed reinforced concrete columns to reduce post-earthquake residual displacements of bridges." *5th National Seismic Conf. on Bridges and Highways*, San Francisco, CA.

Makris, N. (1997). "Rigidity-plasticity–Viscosity: Can electrorheological dampers protect base-isolated structures from near-source ground motions?" *Earthquake Eng. Struct. Dyn.*, 26(5), 571–591.

Makris, N., and Black, C. J. (2002). "Uplifting and overturning of equipment anchored to a base foundation." *Earthquake Spectra*, 18(4), 631–661.

Makris, N., and Black, C. J. (2004a). "Dimensional analysis of bilinear oscillators under pulse-type excitations." *J. Eng. Mech.*, 10.1061/(ASCE)0733-9399(2004)130:9(1019), 1019–1031.

Makris, N., and Black, C. J. (2004b). "Dimensional analysis of rigid-plastic and elastoplastic structures under pulse-type excitations." *J. Eng. Mech.*, 10.1061/(ASCE)0733-9399(2004)130:9(1006), 1006–1018.

Makris, N., and Chang, S.-P. (2000). "Effect of viscous, viscoplastic and friction damping on the response of seismic isolated structures." *Earthquake Eng. Struct. Dyn.*, 29(1), 85–107.

Makris, N., and Kampas, G. (2013). "Estimating the 'effective period' of bilinear systems with linearization methods, wavelet and time-domain analyses: From inelastic displacements to modal identification." *Soil Dyn. Earthquake Eng.*, 45, 80–88.

Makris, N., Kampas, G., and Angelopoulou, D. (2010). "The eigenvalues of isolated bridges with transverse restraints at the end abutments." *Earthquake Eng. Struct. Dyn.*, 39(8), 869–886.

Makris, N., and Psychogios, T. (2006). "Dimensional response analysis of yielding structures with first-mode dominated response." *Earthquake Eng. Struct. Dyn.*, 35(10), 1203–1224.
Makris, N., and Vassiliou, M. F. (2013). "Planar rocking response and stability analysis of an array of free-standing columns capped with a freely supported rigid beam." *Earthquake Eng. Struct. Dyn.*, 42(3), 431–449.
Makris, N., and Vassiliou, M. F. (2014). "Are some top-heavy structures more stable?" *J. Struct. Eng.*, 10.1061/(ASCE)ST.1943-541X.0000933, 06014001.
Makris, N., and Zhang, J. (2001). "Rocking response of anchored blocks under pulse-type motions." *J. Eng. Mech.*, 10.1061/(ASCE)0733-9399(2001)127:5(484), 484–493.
Makris, N., and Zhang, J. (2004). "Seismic response analysis of a highway overcrossing equipped with elastomeric bearings and fluid dampers." *J. Struct. Eng.*, 10.1061/(ASCE)0733-9445(2004)130:6(830), 830–845.
Mander, J. B., and Cheng, C. T. (1999). "Replaceable hinge detailing for bridge columns." *ACI J.*, 187, 185–204.
Mavroeidis, G. P., and Papageorgiou, A. S. (2003). "A mathematical representation of near-fault ground motions." *Bull. Seism. Soc. Am.*, 93(3), 1099–1131.
Milne, J. (1885). "Seismic experiments." *Trans. Seismol. Soc. Jpn.*, 8, 1–82.
Palermo, A., Pampanin, S., and Calvi, G. M. (2005). "Concept and development of hybrid solutions for seismic resistant bridge systems." *J. Earthquake Eng.*, 9(6), 899–921.
Pampanin, S. (2005). "Emerging solutions for high seismic performance of precast/prestressed concrete buildings." *J. Adv. Concr. Technol.*, 3(2), 207–223.
Priestley, M. N., and Tao, J. R. (1993). "Seismic response of precast prestressed concrete frames with partially debonded tendons." *PCI J.*, 38(1), 58–69.
Ricker, N. (1943). "Further developments in the wavelet theory of seismogram structure." *Bull. Seismol. Soc. Am.*, 33(3), 197–228.
Ricker, N. (1944). "Wavelet functions and their polynomials." *Geophys.*, 9(3), 314–323.
Sakai, J., Jeong, H., and Mahin, S. A. (2006). "Reinforced concrete bridge columns that re-center following earthquakes." *Proc. 8th US National Conf. on Earthquake Engineering*, 18–22.
Vassiliou, M. F. (2010). "Analytical investigation of the dynamic response of a pair of columns capped with a rigid beam and of the effect of seismic isolation on rocking structures." Doctoral dissertation, Dept. of Civil Engineering, Univ. of Patras, Greece (in Greek).
Vassiliou, M. F., Mackie, K. R., and Stojadinović, B. (2014). "Dynamic response analysis of solitary flexible rocking bodies: Modeling and behavior under pulse-like ground excitation." *Earthquake Eng. Struct. Dyn.*, 43(10), 1463–1481.
Vassiliou, M. F., and Makris, N. (2011). "Estimating time scales and length scales in pulselike earthquake acceleration records with wavelet analysis." *Bull. Seismol. Soc. Am.*, 101(2), 596–618.
Vassiliou, M. F., and Makris, N. (2012). "Analysis of the rocking response of rigid blocks standing free on a seismically isolated base." *Earthquake Eng. Struct. Dyn.*, 41(2), 177–196.
Veletsos, A. S., and Newmark, N. M. (1960). "Effect of inelastic behavior on the response of simple systems to earthquake motions." *Proc., 2nd World Conf. on Earthquake Engineering*, Tokyo, Japan, 895–912.
Veletsos, A. S., Newmark, N. M., and Chelepati, C. V. (1965). "Deformation spectra for elastic and elastoplastic systems subjected to ground shock and earthquake motions." *Proc., 3rd World Conf. on Earthquake Engineering*, Vol. II, Wellington, New Zealand, 663–682.
Wacker, J. M., Hieber, D. G, Stanton, J. F., and Eberhard, M. O. (2005). "Design of precast concrete piers for rapid bridge construction in seismic regions." *Research Rep.*, Federal Highway Administration, Washington, DC.
Zhang, J., Makris, N., and Delis, T. (2004). "Structural characterization of modern highway overcrossings-case study." *J. Struct. Eng.*, 10.1061/(ASCE)0733-9445(2004)130:6(846), 846–860.